

# Search for the low-lying SUSY spectrum at the LHC consistent with the recent muon $g - 2$ result

Amin Aboubrahim

Institut für Theoretische Physik, Westfälische Wilhelms-Universität  
Münster, Germany

The XXVIII International Conference on Supersymmetry and  
Unification of Fundamental Interactions (SUSY 2021)

Beijing, China (Online)  
August 23 to August 28, 2021

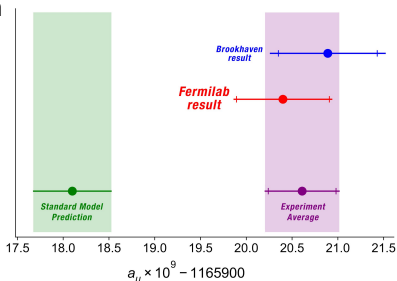
## Table of Contents

- 1 Fermilab  $g - 2$  result
- 2 Supersymmetric loop contributions to  $g - 2$
- 3 Scan of SUGRA parameter space with ML
- 4 Sparticle mass hierarchies
- 5 LHC analysis using a deep neural network
- 6 Conclusions

Fermilab E989 experiment has measured  $a_\mu = (g - 2)_\mu/2$  with an unprecedented accuracy so that

$$a_\mu^{\text{exp}} = 116592040(54) \times 10^{-11}$$

B. Abi *et al.* [Muon  $g-2$ ], *Phys. Rev. Lett.* **126**, no.14, 141801 (2021)

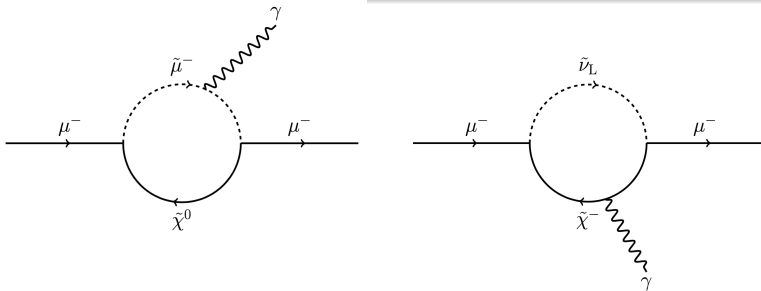


The difference between the combined Fermilab and Brookhaven (FB) result and the SM result is

$$\Delta a_\mu^{\text{FB}} = a_\mu^{\text{exp}} - a_\mu^{\text{SM}} = 251(59) \times 10^{-11},$$

which is a **4.2 $\sigma$  deviation** of experiment from the SM result

# Electroweak SUSY corrections



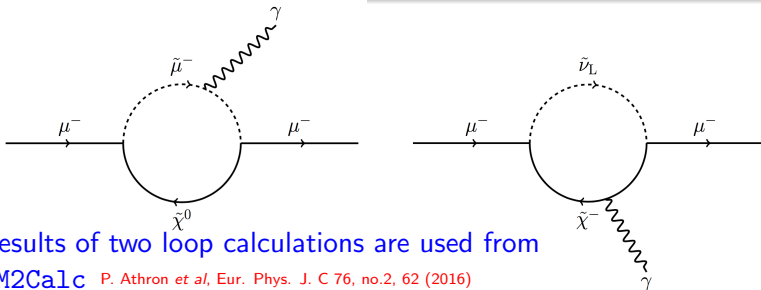
SUGRA unified models can generate SUSY loop corrections to  $(g - 2)_\mu$

$$a_\mu^{\chi^0} = \frac{m_\mu \alpha_{EM}}{4\pi \sin^2 \theta_W} \sum_{j=1}^4 \sum_{k=1}^2 \frac{1}{m_{\tilde{\chi}_j^0}} \left[ \text{Re}(\eta_{\mu j}^k) F_1 \left( \frac{m_{\tilde{\mu}_k}^2}{m_{\tilde{\chi}_j^0}^2} \right) + \frac{m_\mu}{6m_{\tilde{\chi}_j^0}} \chi_{\mu j}^k F_2 \left( \frac{m_{\tilde{\mu}_k}^2}{m_{\tilde{\chi}_j^0}^2} \right) \right]$$

T. Ibrahim and P. Nath,  
 Phys. Rev. D 62, 015004 (2000)

$$a_\mu^{\chi_i^+} = \frac{m_\mu \alpha_{EM}}{4\pi \sin^2 \theta_W} \sum_{i=1}^2 \frac{1}{m_{\tilde{\chi}_i^+}} \left[ \text{Re}(\kappa_\mu U_{i2}^* V_{i1}^*) F_3 \left( \frac{m_{\tilde{\nu}}^2}{m_{\tilde{\chi}_i^+}^2} \right) + \frac{m_\mu}{6m_{\tilde{\chi}_i^+}} (|\kappa_\mu U_{i2}^*|^2 + |V_{i1}|^2) F_4 \left( \frac{m_{\tilde{\nu}}^2}{m_{\tilde{\chi}_i^+}^2} \right) \right]$$

# Electroweak SUSY corrections



Results of two loop calculations are used from

**GM2Calc** P. Athron et al, Eur. Phys. J. C 76, no.2, 62 (2016)

SUGRA unified models can generate SUSY loop corrections to  $(g - 2)_\mu$

$$a_\mu^{\chi^0} = \frac{m_\mu \alpha_{EM}}{4\pi \sin^2 \theta_W} \sum_{j=1}^4 \sum_{k=1}^2 \frac{1}{m_{\tilde{\chi}_j^0}} \left[ \text{Re}(\eta_{\mu j}^k) F_1 \left( \frac{m_{\tilde{\mu}_k}^2}{m_{\tilde{\chi}_j^0}^2} \right) + \frac{m_\mu}{6m_{\tilde{\chi}_j^0}} \chi_{\mu j}^k F_2 \left( \frac{m_{\tilde{\mu}_k}^2}{m_{\tilde{\chi}_j^0}^2} \right) \right]$$

T. Ibrahim and P. Nath,  
Phys. Rev. D 62, 015004 (2000)

$$a_\mu^{\chi_i^+} = \frac{m_\mu \alpha_{EM}}{4\pi \sin^2 \theta_W} \sum_{i=1}^2 \frac{1}{m_{\chi_i^+}} \left[ \text{Re}(\kappa_{\mu} U_{i2}^* V_{i1}^*) F_3 \left( \frac{m_{\tilde{\nu}}^2}{m_{\chi_i^+}^2} \right) + \frac{m_\mu}{6m_{\chi_i^+}} (|\kappa_{\mu} U_{i2}^*|^2 + |V_{i1}|^2) F_4 \left( \frac{m_{\tilde{\nu}}^2}{m_{\chi_i^+}^2} \right) \right]$$

## SUGRA models

- SUGRA high scale model is characterized by five input parameters:  $m_0, A_0, m_{1/2}, \tan \beta, \text{sgn}(\mu)$ . Gaugino sector may be relaxed so one can easily allow for coannihilation

$$m_0, A_0, \boxed{m_1, m_2, m_3}, \tan \beta, \text{sgn}(\mu)$$

- RGE running down to the electroweak scale will generate the entire MSSM sparticle spectrum
- How are the SUGRA input parameters constrained following the recent  $g - 2$  result?
- Can the resulting SUSY spectrum be observable at the LHC?

## Scan with an artificial neural network (ANN)

- We scan the SUGRA parameter space using an ANN
- The ANN has three layers with 25 neurons per layer. It constructs the likelihood of a point using the three constraints on the Higgs mass, DM relic density and muon  $g - 2$ , i.e.,

$$m_{h^0} = 125 \pm 2 \text{ GeV},$$

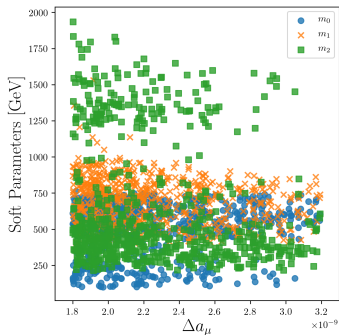
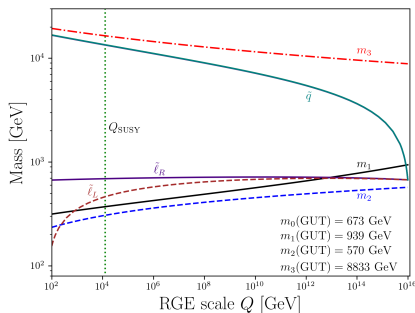
$$\Omega h^2 < 0.126,$$

$$\Delta a_\mu = (2.87 \pm 0.97) \times 10^{-9}.$$

- It is observed that the allowed regions of the parameter space are those where **gluino-driven radiative breaking of the electroweak symmetry** occurs

# RGE running and soft parameters consistent with $(g - 2)_\mu$

[AA, M. Klasen, P. Nath and R. M. Syed, [arXiv:2107.06021 [hep-ph]]].

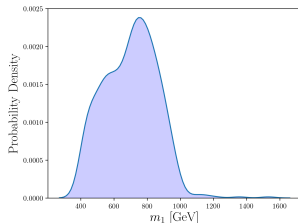
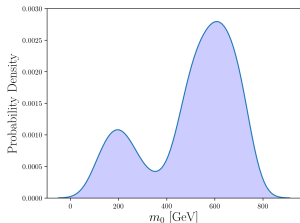


Glauino-driven EWSB: Large  $m_3$  leading to heavy colored sector particles

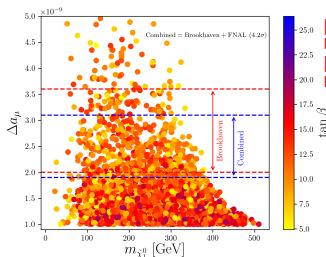
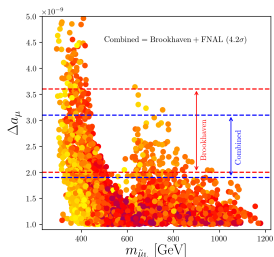
The electroweak sector remains light and within reach of the LHC



# Input parameters and sparticle spectrum



Consistent with:  
 Higgs boson mass,  
 DM relic density, DM  
 direct detection  
 experiments and LHC  
 limits on sparticles



[AA, M. Klasen and P. Nath, [arXiv:2104.03839 [hep-ph]] (to appear in PRD)].

The light sparticle spectrum falls in 3 classes of mass hierarchies:

**(A):** Here  $\tilde{\chi}_2^0, \tilde{\chi}_1^\pm$  are essentially degenerate, and  $\tilde{\tau}_1$  is the NLSP.

This leads to the mass hierarchy  $m_{\tilde{\tau}_1} < m_{\tilde{\chi}_2^0}, m_{\tilde{\chi}_1^\pm} < m_{\tilde{\ell}}$

**(B):** Here there is a reversal in the hierarchy for the first two inequalities, i.e., between  $\tilde{\tau}_1$  and  $\tilde{\chi}_2^0$  or  $\tilde{\chi}_1^\pm$

$$m_{\tilde{\chi}_2^0}, m_{\tilde{\chi}_1^\pm} < m_{\tilde{\tau}_1} < m_{\tilde{\ell}},$$

$$m_{\tilde{\chi}_1^\pm} < m_{\tilde{\chi}_2^0} < m_{\tilde{\tau}_1} < m_{\tilde{\ell}},$$

$$m_{\tilde{\chi}_1^\pm} < m_{\tilde{\tau}_1} < m_{\tilde{\chi}_2^0} < m_{\tilde{\ell}}.$$

**(C):** In this case the sleptons are lighter than  $\tilde{\chi}_1^\pm$  and  $\tilde{\chi}_2^0$  while the stau is the NLSP. Thus here we have  $m_{\tilde{\tau}_1} < m_{\tilde{\ell}} < m_{\tilde{\chi}_2^0}, m_{\tilde{\chi}_1^\pm}$

- We select the set of benchmarks

|     | Model | $h^0$ | $\tilde{\ell}_L$ | $\tilde{\ell}_R$ | $\tilde{\nu}_L$ | $\tilde{\tau}_1$ | $\tilde{\chi}_1^0$ | $\tilde{\chi}_1^\pm$ | $\Omega h^2$ | $\Delta a_\mu (\times 10^{-9})$ |
|-----|-------|-------|------------------|------------------|-----------------|------------------|--------------------|----------------------|--------------|---------------------------------|
| (A) | (a)   | 123.0 | 508.1            | 762.0            | 502.3           | 331.9            | 324.2              | 404.3                | 0.004        | 2.11                            |
| (B) | (b)   | 123.4 | 305.0            | 463.0            | 295             | 251.7            | 237.4              | 237.6                | 0.002        | 2.33                            |
|     | (c)   | 123.7 | 346.8            | 511.9            | 338.0           | 240.3            | 205.6              | 205.8                | 0.001        | 2.67                            |
|     | (d)   | 125.3 | 422.8            | 763.8            | 415.7           | 370.4            | 337.3              | 337.6                | 0.003        | 2.14                            |
| (C) | (e)   | 124.5 | 628.7            | 402.2            | 623.6           | 338.3            | 326.8              | 998.4                | 0.082        | 1.94                            |
|     | (f)   | 123.4 | 722.8            | 262.9            | 718.2           | 206.5            | 195.5              | 1038.4               | 0.103        | 2.57                            |
|     | (g)   | 123.9 | 856.4            | 327.4            | 852.4           | 243.5            | 240.1              | 1227                 | 0.016        | 1.94                            |

- LHC production and decay

$$\left. \begin{aligned}
 pp &\rightarrow \tilde{\ell}_{L/R} \tilde{\ell}_{L/R} \rightarrow l^+ l^- \tilde{\chi}_1^0 \tilde{\chi}_1^0 \\
 pp &\rightarrow \tilde{\nu}_L \tilde{\nu}_L \rightarrow \tilde{\chi}_1^+ \tilde{\chi}_1^- l^+ l^- \\
 pp &\rightarrow \tilde{\nu}_L \tilde{\ell}_L \rightarrow \tilde{\chi}_1^0 \tilde{\chi}_1^+ l^+ l^-
 \end{aligned} \right\} \text{SFOS leptons + MET}$$

- We use a **deep neural network (DNN)** to train the signal and background events using a set of kinematic variables

$$E_T^{\text{miss}}, \quad p_T(j_1), \quad p_T(\ell_1), \quad p_T(\ell_2), \quad p_T^{\text{ISR}}, \quad M_{T2}, \quad M_T^{\text{min}}, \quad m_{\ell\ell}, \\ \Delta\phi(\mathbf{p}_T^\ell, \mathbf{p}_T^{\text{miss}}), \quad \Delta\phi_{\text{min}}(\mathbf{p}_T(j_i), \mathbf{p}_T^{\text{miss}}),$$

where  $M_T^{\text{min}} = \min[m_T(\mathbf{p}_T^{\ell_1}, \mathbf{p}_T^{\text{miss}}), m_T(\mathbf{p}_T^{\ell_2}, \mathbf{p}_T^{\text{miss}})]$

- The DNN employed has **three dense hidden layers with 128 neurons per layer and tanh as an activation function** to define the output neurons given the input values [TMVA: P. Speckmayer, A. Hocker, J. Stelzer and H. Voss, J. Phys. Conf. Ser. 219, 032057 (2010)]
- We consider two signal regions: SR-2 $\ell$ 1j (one non-b-tagged jet) and SR-2 $\ell$ 2j (at least two non-b-tagged jets)

# Kinematic cuts

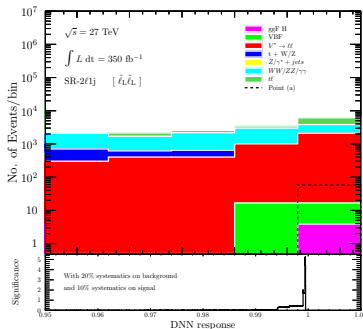
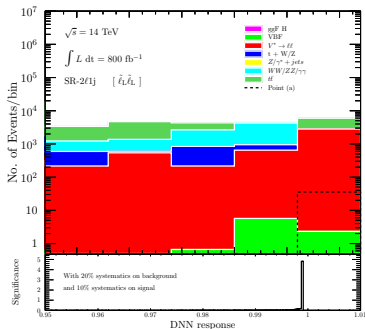
## Cuts are customized for HL-LHC and HE-LHC

| Observable   | (b), (c), (d)                          | (a)          | (e), (f), (g) | (b), (c), (d)                          | (a)          | (e), (f), (g) |
|--|--|--------------|---------------|--|--------------|---------------|
|  | Preselection criteria (SR-2 $\ell$ 2j) |              |               | Preselection criteria (SR-2 $\ell$ 1j) |              |               |
| $N_\ell$ (SFOS)  |  | 2            |               |  | 2            |               |
| $N_{\text{jets}}^{\text{non-b-tagged}}$                                      |  | $\geq 2$     |               |  | 1            |               |
| $p_T(j_1)$ [GeV]   |  | $> 20$       |               |  | $> 20$       |               |
| $p_T(\ell_1)$ (electron, muon) [GeV]   |  | $> 15, > 10$ |               |  | $> 15, > 10$ |               |
| $E_T^{\text{miss}}$ [GeV]  |  | $> 100$      |               |  | $> 100$      |               |
|  | Analysis cuts                          |              |               | Analysis cuts                          |              |               |
| $m_{\ell\ell}$ [GeV] $>$   | 136 (110)                              | 150          | 150 (110)     | 110                                    | 120          | 150           |
| $E_T^{\text{miss}}/p_T^\ell >$   | 1.9 (2.8)                              | -            | -             | 1.0                                    | -            | -             |
| $\Delta\phi_{\min}(\mathbf{p}_T(j_i), \mathbf{p}_T^{\text{miss}})$ [rad] $>$ | -                                      | 0.85 (1.5)   | -             | -                                      | 0.85 (1.5)   | -             |
| $p_T(\ell_2)$ [GeV] $>$  | -                                      | -            | 190 (370)     | -                                      | -            | 190 (300)     |
| $M_{T2}$ [GeV] $>$   | - (140)                                | - (120)      | 200 (300)     | 130 (230)                              | 100          | 200 (300)     |
| DNN response $>$   | 0.95                                   | 0.95         | 0.95          | 0.95                                   | 0.95         | 0.95          |

# Signal and background distributions 1/2

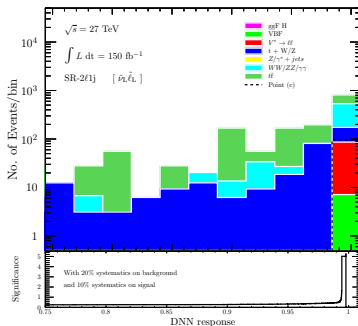
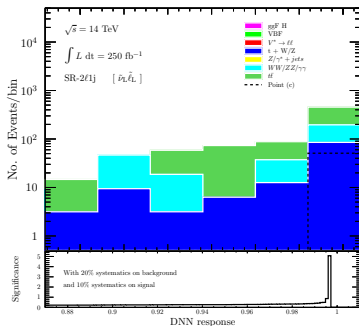
Distributions of  $S$  and  $B$  for the **di-slepton** channel and signal region SR-2 $\ell$ 1j at 14 TeV and 27 TeV

[20% systematics included in the background and 10% in the signal]

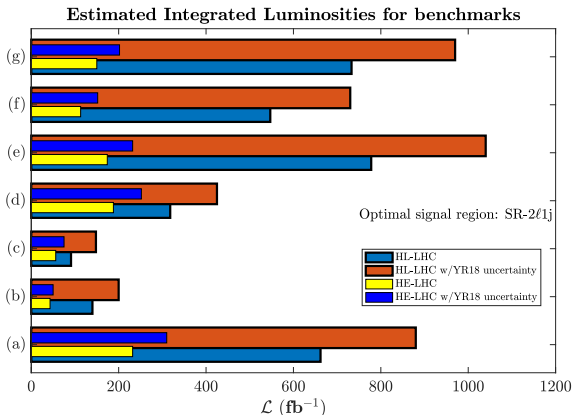


## Signal and background distributions 2/2

Distributions of  $S$  and  $B$  for the **neutrino-slepton** channel and signal region SR- $2\ell 1j$  at 14 TeV and 27 TeV  
 [20% systematics included in the background and 10% in the signal]



# Integrated luminosities for the combined channels



Benchmarks (b) and (c) require  $200 \text{ fb}^{-1}$  and  $148 \text{ fb}^{-1}$  at 14 TeV. The rest require more than  $400 \text{ fb}^{-1}$  but are all within the reach of HL-LHC. Much smaller integrated luminosities are required for HE-LHC

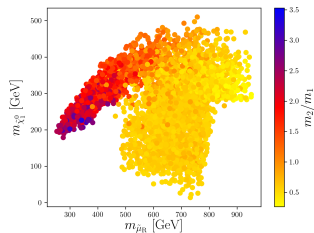
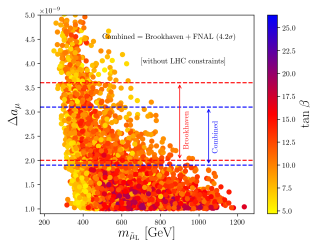
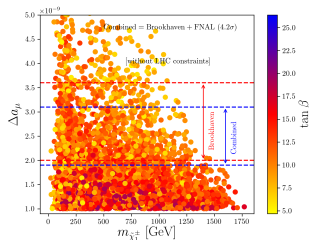
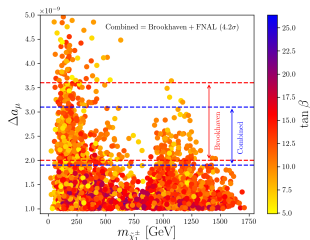


## Conclusions

- A scan of the SUGRA parameter space using ML while imposing the recent  $(g - 2)_\mu$  result naturally leads to the case of gluino-driven EWSB
- The colored sparticles are heavy while the electroweak sector is low-lying and within reach of the LHC
- The mean light sparticle masses are:  $m_{\tilde{\chi}_1^0} \sim 235$  GeV,  $m_{\tilde{\chi}_1^\pm} \sim 445$  GeV,  $m_{\tilde{\ell}_L} \sim 480$  GeV,  $m_{\tilde{\ell}_R} \sim 590$  GeV,  $m_{\tilde{\nu}_L} \sim 470$  GeV and  $m_{\tilde{\tau}_1} \sim 300$  GeV
- We studied slepton and sneutrino pair production as well as slepton-sneutrino associated production
- Some benchmarks can be discovered in the next run of HL-LHC while lower integrated luminosities are required at HE-LHC

# BACKUP SLIDES

# Results of the scan with ANN



The left and right smuon masses at one loop so that

$$m_{\tilde{\mu}_L}^2 = m_0^2 + m_\mu^2 + C_1 m_1^2 + C_2 m_2^2 + \left(-\frac{1}{2} + \sin^2 \theta_W\right) M_Z^2 \cos(2\beta)$$

$$m_{\tilde{\mu}_R}^2 = m_0^2 + m_\mu^2 + 4C_1 m_1^2 - \sin^2 \theta_W M_Z^2 \cos(2\beta)$$

Here  $C_1 = \frac{3}{10} \tilde{\alpha}_G f_1$ ,  $C_2 = \frac{3}{2} \tilde{\alpha}_G f_2$ , where  $\tilde{\alpha}_G = \alpha_G / (4\pi)$ ,  
 $f_k(t) = t(2 + b_k \tilde{\alpha}_G t) / (1 + b_k \tilde{\alpha}_G t)^2$ ,  $t = \ln(M_G^2 / Q^2)$  and  
 $(b_1, b_2) = (33/5, 1)$ . Thus

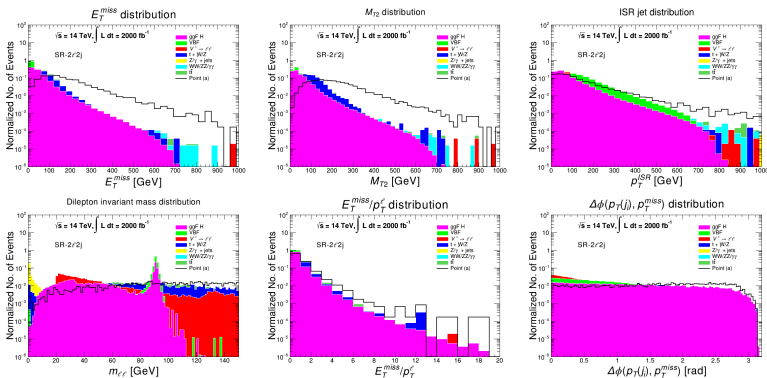
$$m_{\tilde{\mu}_R}^2 - m_{\tilde{\mu}_L}^2 = 3m_1^2 C_1 - m_2^2 C_2 + \left(\frac{1}{2} - 2 \sin^2 \theta_W\right) M_Z^2 \cos(2\beta)$$

Using  $\alpha_1 \sim 0.016$ ,  $\alpha_2 = 0.033$ ,  $\alpha_G \sim 0.04$  and  $M_G \sim 1.2 \times 10^{16}$  GeV gives  $C_1 \approx 0.16$  and  $C_2 \approx 0.23$ . Thus one finds that typically the right smuon has a larger mass than the left smuon unless

$m_2 \gtrsim 1.24 m_1$  (with the assumed input)



# Kinematic variables used for training DNN



We use the signal significance  $Z = \frac{S}{\sqrt{S + B + (\delta_S S)^2 + (\delta_B B)^2}}$  to determine the required integrated luminosity for discovery  $\mathbb{E}$

- We determine the angle between the dilepton system and each non-b-tagged jet in the event, i.e.,  $\Delta\phi(p_T(j_i), p_T^\ell)$
- If an event has **exactly two jets** with  $p_T(j_1)$  and  $p_T(j_2)$ , respectively, then
  - ① if  $\Delta\phi(p_T(j_1), p_T^\ell) < \Delta\phi(p_T(j_2), p_T^\ell)$ , both are tagged as non-ISR jets
  - ② if  $\Delta\phi(p_T(j_1), p_T^\ell) > \Delta\phi(p_T(j_2), p_T^\ell)$ , then the subleading jet is tagged as non-ISR and the leading one will be an ISR jet
- If an event has more than two jets, then we select **up to two** jets that are closest to the dilepton system and tag them as non-ISR (possible jets arising from the decay of the SUSY system) and the rest are classified as ISR jets

The largest number of events correspond to the case of one ISR and one non-ISR jet per event. Moreover, one can get as many as six ISR jets in an event but with a low event count while a larger number of events have no ISR jets.

## LHC production cross sections

**Table:** The aNNLO+NNLL production cross-sections of slepton pair ( $\tilde{\ell} = \tilde{e}, \tilde{\mu}$ ) and sneutrino pair as well as slepton associated production with a sneutrino at  $\sqrt{s} = 14$  TeV and  $\sqrt{s} = 27$  TeV for our benchmarks. The cross section is in fb.

| Model | $\sigma(pp \rightarrow \tilde{\ell}_L \tilde{\ell}_L)$ |        | $\sigma(pp \rightarrow \tilde{\ell}_R \tilde{\ell}_R)$ |        | $\sigma(pp \rightarrow \tilde{\nu}_L \tilde{\ell}_L)$ |        | $\sigma(pp \rightarrow \tilde{\nu}_L \tilde{\nu}_L)$ |        |
|-------|--|--------|--|--------|---|--------|--|--------|
|       | 14 TeV   | 27 TeV | 14 TeV   | 27 TeV | 14 TeV  | 27 TeV | 14 TeV   | 27 TeV |
| (a)   | 1.084  | 4.515  | 0.057  | 0.335  |   |        |  |        |
| (b)   | 9.810  | 30.80  | 0.656  | 2.54   | 41.78   | 127.80 | 10.52  | 33.10  |
| (c)   | 5.805  | 19.31  | 0.417  | 1.72   | 24.40   | 78.97  | 4.94   | 15.10  |
| (d)   | 2.486  | 9.188  | 0.056  | 0.332  | 10.44   | 37.47  | 2.10   | 7.21   |
| (e)   | 0.388  | 1.915  | 1.22   | 4.32   |   |        |  |        |
| (f)   | 0.188  | 1.065  | 6.91   | 20.15  |   |        |  |        |
| (g)   | 0.074  | 0.506  | 2.87   | 9.22   |   |        |  |        |



## Estimated integrated luminosity for discovery

**Table:** The estimated integrated luminosities, in  $\text{fb}^{-1}$ , for discovery of our benchmarks at 14 TeV and 27 TeV after combining all production channels and including systematics in the signal and background.

| Model | SR-2 $l$ 1j             |                         | SR-2 $l$ 2j             |                         |
|-------|-------------------------|-------------------------|-------------------------|-------------------------|
|       | $\mathcal{L}$ at 14 TeV | $\mathcal{L}$ at 27 TeV | $\mathcal{L}$ at 14 TeV | $\mathcal{L}$ at 27 TeV |
| (a)   | 880                     | 310                     | 1262                    | 694                     |
| (b)   | 200                     | 50                      | 1860                    | 715                     |
| (c)   | 148                     | 75                      | 1887                    | 1320                    |
| (d)   | 425                     | 252                     | ...                     | 2804                    |
| (e)   | 1040                    | 232                     | 1738                    | 1194                    |
| (f)   | 730                     | 152                     | 2074                    | 689                     |
| (g)   | 970                     | 202                     | ...                     | 1031                    |

## The 27 TeV collider: HE-LHC

- The High Energy LHC (HE-LHC) is a possible candidate as the next generation  $pp$  collider at CERN
- Uses the existing LHC ring with 16 T FCC magnets replacing the current 8.3 T ones
- Center-of-mass energy boosted to 27 TeV with a design luminosity  $\sim 5$  times that of the HL-LHC
- This set up necessarily means that a larger part of the parameter space of supersymmetric models beyond the reach of the 14 TeV collider will be probed